Three-dimensional Quantum Cellular Neural Network and Its Application to Image Processing *

Sen Wang, Li Cai, Huanqing Cui, Chaowen Feng, Xiaokuo Yang
Science College, Air Force Engineering University
Xi'an 710051, China
wangsen1998-2002@163.com

***Abstract*—A three-dimensional quantum cellular neural network is proposed by using the quantum cellular automata as neuron cells. The three-dimensional quantum cellular neural network consists of two layers of quantum cellular automata array and possesses the A cloning template, B cloning template, and threshold. The image processing functions such as hole filling and corner detecting were performed by using the polarization of quantum cellular automata as pixel value and selecting different cloning templates and thresholds. The SIMULINK model is employed to simulate image processing functions and the simulation results demonstrate the effectiveness of the proposed quantum cellular neural networks.**

Keywords—image processing; quantum cellular neural network; cellular neural network; quantum cellular automata

I. INTRODUCTION

The real-time image processing of large size images on a general-purpose computer is a time and resource consuming task. It would be of great practical benefit to develop high-parallel data processing hardware[1].

Cellular neural networks (CNN) have attracted plenty of interest as a promising architecture for parallel data processing[2-3]. However, hardware implementation of CNN has always been challenging in terms of power consumption and integration density. The neuron cells in CNN are mainly constructed by large number of transistors in prior work, and result in high power consumption and low packing density.

A quantum cellular neural network (QCNN) model[4-5] has been proposed, in which neuron cells are constructed by quantum cellular automata (QCA)[6]. QCNNs represent innovative architectures in the field of CNNs, and possess the advantages of the QCAs and CNNs, whose peculiarities lie in the extremely high packing density, ultra low power consumption, and simplified interconnection.

Recently, QCNNs are used to realize ultra-small chaotic generators for control and secure communication[7-10]. Additionally, in [11], two-dimensional QCNNs are proposed and applied to image processing. However, the image processing functions of the two-dimensional QCNNs are more simple, because it can only realize the A cloning template of CNNs. In this paper, A three-dimensional QCNN is proposed. The new structure of the QCNN contains two layers of QCA array and possesses the A cloning template, B cloning template, and threshold. Hole filling operation and corner detecting operation are performed by selecting different cloning templates and thresholds. This study could be very important for future ultra-high density realization and applications of CNNs.

II. THREE-DIMENSIONAL QUANTUM CELLULAR NEURAL NETWORKS

The neuron cells in QCNNs are constructed by QCAs. A QCA consists of an array of quantum-dots and tunnel junctions. Quantum-dots are connected locally by the interactions of the electrons contained in Quantum-dot[6]. Electrons can tunnel between the quantum dots in the same cell through tunnel junctions. The electrons tend to occupy antipodal sites within the cell due to their mutual electrostatic repulsion, thus an isolated cell possesses two complete polarized states as shown in Fig. 1.

The architecture of QCNN is similar to that of CNN, and the interaction between neighboring cells is not by connecting wires but by Coulomb force. Fig. 2 shows the structure of three-dimensional QCNN.

In Fig. 2, blocks represent QCA cells, top QCA array is input layer, and bottom QCA array is output layer. The input layer accepts data input and the value of cells are fixed when QCNNs evolve. The value of output layer cells will vary based on the input and output layer cells.

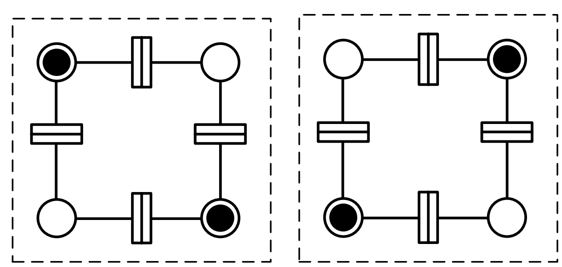

Fig. 1 The two complete polarized states of QCA

This work was supported by the National Natural Science Foundation of China (grant nos. 61401498), and the Program of Shaanxi Provincial Natural Science for Basic Research (grant no. 2014JQ8343)

978-1-5090-5507-4/17/$31.00 ©2017 IEEE
ICIS 2017, May 24-26, 2017, Wuhan, China

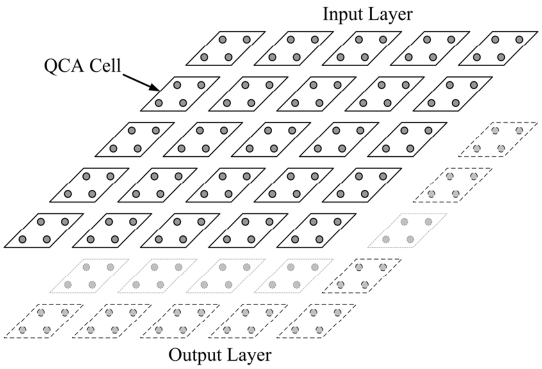

Fig. 2 The structure of the three-dimensional QCNN

QCNNs can be described by a set of state variables which contains the classical cell polarization P and a quantum phase angle φ. The dynamics of the output layer cell k can be described as follows [12]

$$\begin{aligned} \hbar \frac{\mathrm{d}P_k}{\mathrm{d}t} &= -2\gamma\sqrt{1-P_k^2}\sin\varphi_k \\ \hbar \frac{\mathrm{d}\varphi_k}{\mathrm{d}t} &= -E_k \overline{P}_k + 2\gamma \frac{P_k}{\sqrt{1-P_k^2}}\cos\varphi_k \end{aligned} \tag{1}$$

where $\hbar$ is the Planck constant, γ is the inter-dot tunneling energy inside each cell, E_k is the electrostatic energy cost of two adjacent fully polarized cells having opposite polarization, and $\overline{P}_k$ is the weighted sum of the neighboring cells polarization.

Consider an $M \times N$ three-dimensional QCNN, having $M \times N$ cells arranged in M rows and N columns of every layer. We denote the cell on the ith row and jth column by $C(i,j)$. In three-dimensional QCNN, the effect of input layer to output layer need to be taken into account, and the state equation of the cell $C(i,j)$ in output layer can be described as follows

$$\begin{aligned} \frac{\mathrm{d}P_{i,j}}{\mathrm{d}t} &= -2a\sqrt{1-P_{i,j}^2}\sin\varphi_{i,j} \\ \frac{\mathrm{d}\varphi_{i,j}}{\mathrm{d}t} &= -\sum_{C(k,l)\in N_r(i,j)} W(i,j;k,l)P_{k,l} - \sum_{C(k,l)\in N_r(i,j)} U(i,j;k,l)P_{k,l}^{\text{input}} \\ &\quad + 2a\frac{P_{i,j}}{\sqrt{1-P_{i,j}^2}}\cos\varphi_{i,j} + b \end{aligned} \tag{2}$$

where $a = \gamma/\hbar$, $P_{k,l}^{\text{input}}$ is the polarization of input layer cell $C(k,l)$, and b is the threshold of input layer to output layer. $N_r(i,j)$ is the neighborhood of cell $C(i,j)$ and is defined as

$$N_r(i,j) = \left\{ C(k,l) \,\middle|\, \begin{matrix} \max(|i-k|,|j-l|) \le r \\ 1 \le k \le M \\ 1 \le l \le N \end{matrix} \right\} \tag{3}$$

where r is a positive integer denoting the radius of the neighborhood.

$W(i,j;k,l)$ is the weight of output layer cell $C(k,l)$ to output layer cell $C(i,j)$, $U(i,j;k,l)$ is the weight of input layer cell $C(k,l)$ to output layer cell $C(i,j)$. Moreover, all cells on the same layer are assumed to be identical, hence, $W(i,j;k,l)$ and $U(i,j;k,l)$ are independent of i and j. Consequently, the $W(i,j;k,l)$ and $U(i,j;k,l)$ can be expressed as

$$\begin{cases} W(i,j;k,l) = A(k-i,l-j) \\ U(i,j;k,l) = B(k-i,l-j) \end{cases} \tag{4}$$

When r=1, the matrix $\boldsymbol{A}$ and $\boldsymbol{B}$ are 3×3 square arrays as shown in Fig. 3, and are normally called as A and B cloning templates, respectively.

Moreover, the Coulomb interaction between output layer cell $C(k,l)$ and $C(i,j)$ is reciprocal, and is weighted by $W(i,j;k,l)$, hence, we have

$$W(i,j;k,l) = W(k,l;i,j) \tag{5}$$

From (4) and (5), it can be deduced that

$$A(k-i,l-j) = A(i-k,j-l) \tag{6}$$

From (6), it can be derived that the A cloning template is centrosymmetric.

III. Application of Quantum Cellular Neural Networks to Image Processing

In order to apply QCNNs to image processing, it is needed to implement the following procedure in advance:

a) The pixels are constructed by cells in the same layer, and the pixel value is represented by the polarization of the cell.

b) Assume that the pixel values “-1” and “1” correspond to black and white, respectively, and the pixel values between “-1” and “1” correspond to different gray-scale level.

A(-1,-1)	A(-1,0)	A(-1,1)
A(0,-1)	A(0,0)	A(0,1)
A(1,-1)	A(1,0)	A(1,1)

(a)

B(-1,-1)	B(-1,0)	B(-1,1)
B(0,-1)	B(0,0)	B(0,1)
B(1,-1)	B(1,0)	B(1,1)

(b)

Fig. 3 Cloning templates (a) A cloning template; (b) B cloning template

Different image processing function can be acquired by chosen different A , B cloning templates and threshold *b*. In the following numerical calculation, the array of every layer is 30×30 , and other system parameters are chosen as: $a=0.02$, $r=1$.

A. Simulation of Quantum Cellular Neural Networks

The output layer cells' dynamics are described as (2), and the SIMULINK model of cell $C(i,j)$ is shown in Fig.4.

In Fig.4, from "In1" to "In8" are polarizations of neighborhood of output layer cell $C(i,j)$, and from "In9" to "In17" are polarizations of input layer cells. "Out1" is the polarization of the output layer cell $C(i,j)$, and "Out2" is the quantum phase angle of the output layer cell $C(i,j)$. "Threshold" is the threshold *b*, $\mathrm{A}kl\left(\mathrm{k},l=1,2,3\right)$ and $\mathrm{B}kl\left(\mathrm{k},l=1,2,3\right)$ are the A and B cloning templates, respectively. The dynamics behavior of QCNNs can be acquired by connecting the SIMULINK model based on the structure of QCNNs.

B. Hole Filling Operation

When the A and B cloning templates are chosen as Fig. 5, and threshold $b=10$, hole filling operation can be achieved as shown in Fig. 6.

The original image is transmitted to input layer, and the final image is acquired from output layer. From the Fig.6, it can be seen that the inner of "8" was filled by white.

C. Corner Detecting Operation

When the threshold $b=60$,and the A and B cloning templates are chosen as Fig. 7, corner detecting operation can be achieved as shown in Fig. 8 and Fig.9.

5	5	5
5	30	5
5	5	5

(a)

0	0	0
0	30	0
0	0	0

(b)

Fig. 5 "Hole filling" operation template (a) A cloning template; (b) B cloning template

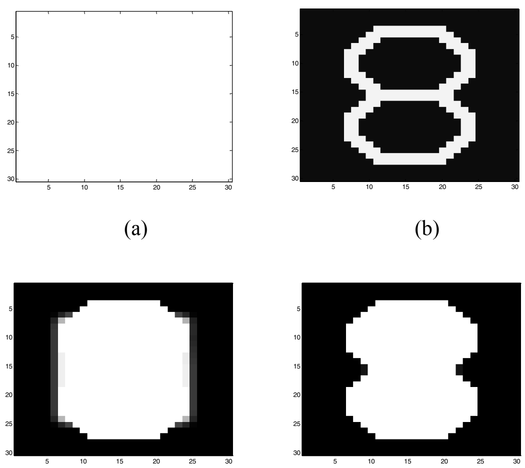

(a) (b) (c) (d)

Fig. 6 Hole filling operation (a) initial image of output layer; (b) input image of input layer; (c) transient image of output layer; (d) steady image of output layer.

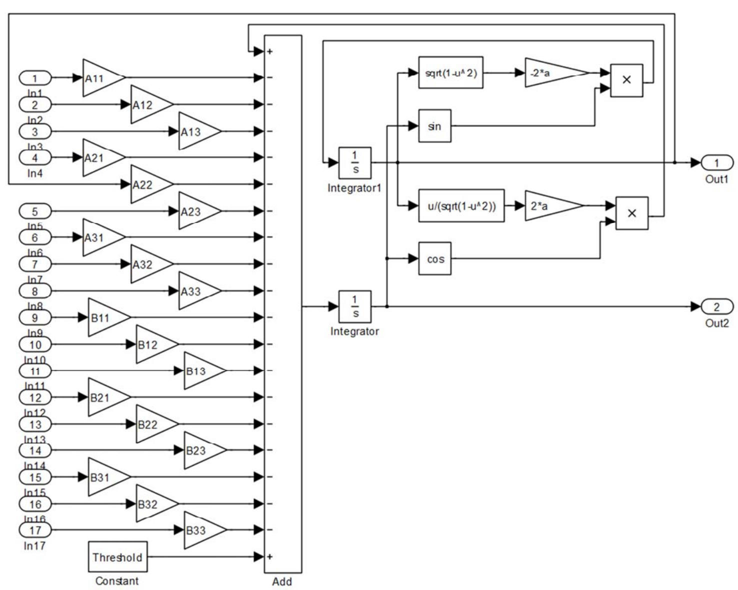

Fig. 4 The SIMULINK model of the output layer cell $C(i,j)$

0	**-5**	**0**
-5	**40**	**-5**
0	**-5**	**0**

(a)

-10	**-10**	**-10**
-10	**40**	**-10**
-10	**-10**	**-10**

(b)

Fig. 7 Corner detecting operation template (a) A cloning template; (b) B cloning template

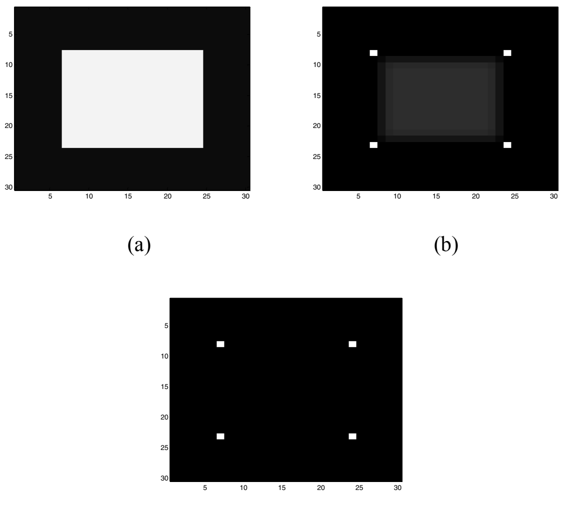

(a) (b) (c)

Fig. 8 Corner detecting operation of square (a) input image of input layer; (b) transient image of output layer; (c) steady image of output layer.

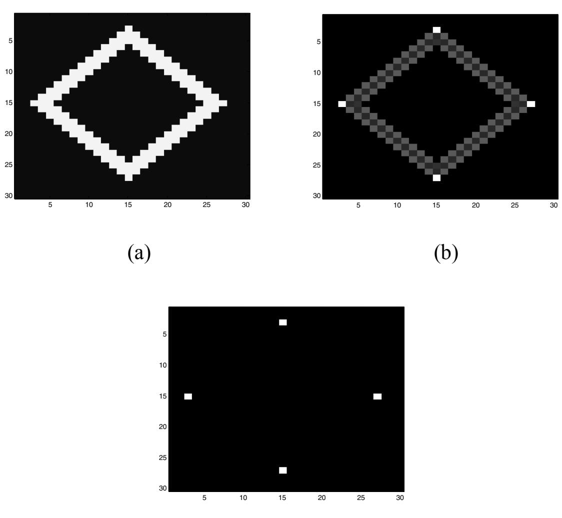

(a) (b) (c)

Fig. 9 Corner detecting operation of diamond (a) input image of input layer; (b) transient image of output layer; (c) steady image of output layer.

In order to implement corner detecting operation, the original image is transmitted to input layer and output layer simultaneously, and the final image is acquired from output layer. From Fig. 8 and Fig. 9, it can be seen that four corner of the square and diamond are detected, respectively.

In [11], we proposed a two-dimensional QCNN which only has the A cloning template. In this paper, the proposed three-dimensional QCNN possesses A cloning template, B cloning template, and threshold. Compared with two-dimensional QCNNs, three-dimensional QCNNs can perform more image processing functions because of the diversity in choosing cloning templates and thresholds. Moreover, when the B cloning template and threshold are set to zero, three-dimensional QCNN is transformed into a two-dimensional QCNN.

IV. Conclusions

This paper proposed a three-dimensional QCNN by using QCAs as neuron cells. The proposed QCNN contains two layers of QCA array and introduces the concepts of A cloning template, B cloning template, and threshold. The functions of the hole filling and corner detecting operation were performed by using the polarization of QCA cell as pixel value and selecting different cloning templates and thresholds. The SIMULINK model is employed to simulate the image processing functions and the simulation results demonstrate the effectiveness of the proposed QCNNs.

Additionally, the QCNNs possesses the advantages of the simplified interconnection, the extremely high packing densities and low power consumption, and will become a very important regime for future evolutions in the field of CNN. The study in this paper provides valuable information about QCNNs for future application in high-parallel signal processing such as image processing and pattern recognition.

References

[1] A. Khitun, M. Q. Bao, and K. L. Wang, “Magnetic cellular nonlinear network with spin wave busfor image processing,” Superlattices and Microstructures, vol. 47, pp. 464-483, November 2010.

[2] L. O. Chua, and L. Yang, “Cellular Neural Networks: Theory,” IEEE Transactions on Circuits and Syestems, vol. 35, pp. 1257-1273, October 1988.

[3] W. Shimoda, and K. Yanai, “CNN-based food image segmentation without pixel-wise annotation,” Lecture Notes in Computer Science, Vol. 9281, pp. 449-457, January 2015.

[4] G. Tóth, C. S. Lent, P. D. Tougaw, Y. Brazhnik, W. Weng, W. Porod, R. W. Liu, and Y.-F. Huang, “Quantum cellular neural networks,” Superlattices Microstructures, vol. 20, pp. 473–478, April 1996.

[5] L. Fortuna, M. L. Rosa, D. Nicolosi, and D. Porto, “Nanoscale system dynamical behaviors: from quantum-dot-based cell to 1-D arrays,” IEEE Transactions on Very Large Scale Integration Syetems, vol. 12, pp. 1167-1173, November 2004.

[6] C. S. Lent, P. D. Tougaw, and G. H. Bernstein, “Quantum cellular automata,” Nanotechnology, vol. 4, pp. 49-57, January 1993.

[7] S. Wang, L. Cai, Q. Kang, G. Wu, and Q. Li, “The characteristics of nonlinear chaotic dynamics in quantum cellular neural networks,” Chinese Physics B, vol. 17, pp. 2837-07, August 2008.

[8] S. Wang, L. Cai, B. Zhang, and H. Y. Zhao, “Chaotic function projective synchronization of quantum cellular neural network,” Micronanoelectronic Technology, vol. 53, pp. 7-12, January 2016(in Chinese)

[9] C. H. Yang, Z. M. Ge, C. M. Chang, and S. Y. Li, “Chaos synchronization and chaos control of quantum-CNN chaotic system by variable structure control and impulse control,” Nonlinear Analysis: Real World Applications, vol. 11, pp. 1977-1985, November 2010.

[10] S. Wang, L. Cai, N. Zhang, C. W. Feng, and X. K. Yang, “Synchronization and multichannel secure communicaiton of quantum cellular neural network,” Proceedings of the 11th World Congress on Intelligent Control and Automation, Shengyang, China, 2014, pp. 4040-4044.

[11] S. Wang, L. Cai, Q. Kang, Q. Li, and G. Wu, “The two-demensional quantum cellular neural network and its applications to image processing,” Research and Progress of solid State Electronics, vol. 28, pp. 340-345, September 2008(in Chinese).

[12] Á. I. Csurgay, W. Porod, and C. S. Lent, “Signal processing with near-neighbor-coupled time-varying quantum-dot arrays,” IEEE Transactions on Circuits and Systems-I: Fundamental Theory and Applications, vol. 47, pp. 1212-1223, August 2000.